Flat bubble regime and laminar plasma flow in a plasma wakefield accelerator

S. S. Baturin*

School of Physics and Engineering, ITMO University, St. Petersburg, Russia 197101

(Received 23 March 2022; accepted 25 July 2022; published 16 August 2022)

A simple 2D model of the bubble formation in a plasma wakefield accelerator is developed and investigated. We show that in the case of a flat driver, the bubble may consist of two parts. The first part corresponds to a laminar flow where plasma electron streams do not cross and the second to the two-stream (turbulent) flow. The laminar flow turns out to be robust to the symmetry breaking. Building off of the developed model, we demonstrate that, in the case of the laminar flow and nonrelativistic plasma electrons, the transverse wakefield is absent inside the bubble even in the case of a transversely nonuniform plasma.

DOI: 10.1103/PhysRevAccelBeams.25.081301

I. INTRODUCTION

The plasma wakefield acceleration (PWA) technique [1–4] attracted much attention over the past several years and is envisioned as one of the main options for the design of future colliders and light sources [5–10].

Development of the PWA emerged into the rapid development of PWA theories from simple yet powerful analytical models [11–15] to complex and precise simulation codes [16–18]. Nonetheless, a significant understanding of physical processes that underlie PWA technology has already been gained, there is still ongoing work on the theoretical side as well as extensive experimental developments (see, for instance, Refs. [19,20]). Several questions such as optimal beam-loading [21], instability suppression, and instability mechanisms [22–25], as well as acceptable tolerances [26], are still under active study.

The main challenge that is common to all wakefield accelerators, be it plasma-based or structure-based (dielectric loaded or corrugated structures [27–29]) machines, is the beam breakup instability that directly affects the efficiency of the accelerator [30–33]. Many mechanisms and approaches were investigated, including ion motion [23] Balakin, Novokhatski, and Smirnov damping [22,24] and other methods of resonance elimination.

One of the approaches that stand aside is the transverse shaping of the driver beam that mainly includes injection of the flat beam (or the beam with the high ellipticity $\sigma_y/\sigma_x \gg 1$) [34–36] and dual driver injection [33,37]. It was predicted [37,38] and recently experimentally demonstrated [39] that a highly elliptic driver can suppress transverse wake in a structure-based wakefield accelerating device. It turns out that an asymmetric driver is a promising approach in the hollow channel plasma as well [40].

Recently, it has been realized that the path toward a real machine unavoidably includes staging of the individual cells and this, in turn, results in tolerances on plasma cell alignments and plasma density uniformity. Indirect evidence of the nonuniformity effects could be found in the results on hollow channel plasma described in Refs. [41,42].

Being motivated by the recent success of the flat beam application and the need for preliminary analysis of the transverse plasma nonuniformity in this paper, we develop a simple analytical model of the blowout plasma regime formed by the infinitely flat driver and investigate how local nonuniformity of the plasma density affects the problem. We demonstrate that, in contrast to the similar cylindrically symmetric problem with the point driver, considered in Refs. [13,14], in the planar case, the plasma has two regimes, namely, a laminar flow and a turbulent flow. We point out that in the case of a laminar flow and nonrelativistic plasma electrons, the transverse wake is absent even in the case of the transversely nonuniform plasma.

The model and results of the presented analysis may serve as a starting point for further investigation of the flat beam injection into the nonuniform plasma and is beneficial for some basic parameter estimations for the ongoing experimental effort at the Argonne Wakefield Accelerator facility [43].

II. BASIC EQUATIONS

In this section, we provide a brief overview of the model used for the calculus and analysis.

*s.s.baturin@gmail.com

A. General formulas

We start from the set of equations derived in Ref. [14]. We use the same convention as the Ref. [14] and we use dimensionless variables: time is normalized to ω_p^{-1}, length to k_p^{-1}, velocities to the speed of light c, and momenta to mc. We also normalize fields to $mc\omega_p/e$, forces to $mc\omega_p$, potentials to mc^2/e, the charge density to $n_0 e$, the plasma density to n_0, and the current density to en_0c. With e being the elementary charge, $e > 0$.

The equation of motion for the plasma electrons reads

$$\frac{d\mathbf{p}}{dt} = \boldsymbol{\nabla}\psi + \hat{\mathbf{z}} \times \mathbf{B}_\perp - \mathbf{v} \times \mathbf{B}, \qquad \frac{d\mathbf{r}}{dt} = \frac{\mathbf{p}}{\gamma}. \tag{1}$$

Here $\mathbf{p}$ is the momentum of the plasma electrons, $\gamma = \sqrt{1+p^2}$ is the relativistic gamma factor of the plasma electrons, $\mathbf{v} = \mathbf{p}/\gamma$ is the velocity, and $\psi = \phi - A_z$ is the pseudopotential that defines the wakefield as

$$E_z = \frac{\partial \psi}{\partial \xi}, \qquad \mathbf{F}_\perp = -\boldsymbol{\nabla}_\perp \psi, \tag{2}$$

and $\boldsymbol{\nabla} = (\partial_x, \partial_y, -\partial_\xi)$. Here $\mathbf{F}_\perp$ is the transverse part of the Lorentz force per unit charge of the test particle and $\xi = t - z$.

Equation (1) have the following integral of motion:

$$\gamma - p_z - \psi = 1, \tag{3}$$

as a consequence, we have

$$1 - v_z = \frac{1+\psi}{\gamma}. \tag{4}$$

In a quasistatic picture, it is convenient to replace the derivative by time t with the derivative by ξ. We use the fact that

$$\frac{d\xi}{dt} = 1 - v_z, \tag{5}$$

consequently, for an arbitrary function $f(\xi)$, we have

$$\frac{df}{dt} = \frac{df}{d\xi}\frac{d\xi}{dt} = (1-v_z)\frac{df}{d\xi} = \frac{1+\psi}{\gamma}\frac{df}{d\xi}. \tag{6}$$

Since in a quasistatic picture momentum of the plasma electron is a function of ξ Eq. (1) with Eq. (6) are reduced to

$$\frac{d\mathbf{p}_\perp}{d\xi} = \frac{\gamma}{1+\psi}\boldsymbol{\nabla}_\perp\psi + \hat{\mathbf{z}} \times \mathbf{B}_\perp - \frac{B_z}{1+\psi}\mathbf{p}_\perp \times \hat{\mathbf{z}}. \tag{7}$$

The equation for the pseudopotential reads

$$\Delta_\perp \psi = (1-v_z)n_e - n_i(x), \tag{8}$$

here n_e is the plasma electron density and $n_i(x)$ is the ion density that depends on the transverse coordinate x. In what follows, we will assume that

$$n_i(x) = 1 + gx, \tag{9}$$

with $g \ll 1$. The last term in the equation above is responsible for the gradient in plasma density along x axis. Equations for the magnetic field are

$$\Delta_\perp B_z = \hat{\mathbf{z}} \cdot (\boldsymbol{\nabla}_\perp \times n_e \mathbf{v}_\perp), \tag{10}$$

$$\Delta_\perp \mathbf{B}_\perp = -\hat{\mathbf{z}} \times \boldsymbol{\nabla}_\perp n_e v_z - \hat{\mathbf{z}} \times \partial_\xi n_e \mathbf{v}_\perp. \tag{11}$$

The final equation that complements equations for the fields is the continuity equation for the plasma given by

$$\partial_\xi[n_e(1-v_z)] + \nabla_\perp \cdot n_e \boldsymbol{v}_\perp = 0. \tag{12}$$

B. 2D approximation

If one assumes that the charge density is uniform and the charge is distributed along the infinite line in the y direction, then the following simplification to the main set of equations could be made. Equation (2) reduces to

$$E_z = \frac{\partial \psi}{\partial \xi}, \qquad F_x = -\frac{d\psi}{dx}, \qquad F_y = 0. \tag{13}$$

Equation for the pseudopotential (8) reads

$$\frac{d^2\psi}{dx^2} = (1-v_z)n_e - n_i, \tag{14}$$

and continuity equation (12) reads

$$\partial_\xi[n_e(1-v_z)] + \frac{d}{dx}n_e v_x = 0. \tag{15}$$

III. SHOCK WAVE

As discussed in detail in Ref. [14], plasma electrons cross an infinitesimally thin layer in which the fields produced by the driver have a delta-function discontinuity

$$\begin{aligned} \mathbf{E}_\perp &= \mathbf{D}\delta(\xi), \\ \mathbf{B}_\perp &= \hat{\mathbf{z}} \times \mathbf{D}\delta(\xi), \end{aligned} \tag{16}$$

with the transverse profile defined by the vector $\mathbf{D} = (D_x, D_y)$.

To solve for the shock wave at $\xi = 0$, we assume that the plasma density in front of the moving driver has a linear gradient

$$n_e^{(0)} = 1 + gx, \tag{17}$$

where the uniform part of the density in the introduced units is 1, g is a constant, and x is the transverse coordinate. At rest, plasma is electrically neutral, consequently, the gradient in density is the same for both ions Eq. (9) and electrons [Eq. (17)]. As before, we assume a small gradient

$$g \ll 1, \tag{18}$$

and use the perturbation theory.

We consider equation for the vector $\mathbf{D}$, which according to Ref. [14], reads

$$\Delta_\perp \mathbf{D} = \frac{n_e^{(0)}}{\gamma_0}\mathbf{D}. \tag{19}$$

If we set $g = 0$, then due to the symmetry, we have $D_y^{(0)} = 0$ and $D_x^{(0)} = D_x^{(0)}(x, \xi)$. This immediately results in the equation for $D_x^{(0)}$ in a form

$$\frac{d^2}{dx^2} D_x^{(0)} = \frac{n_e^{(0)}}{\gamma_0} D_x^{(0)}. \tag{20}$$

With the unmodified plasma density and initial gamma set to unity ($n_e^{(0)} = 1$, $\gamma_0 = 1$) for boundary conditions $D_x(\pm\infty) = 0$, $D_x(x \to \pm 0) = \pm 2\pi\lambda$, where λ is the line charge density of the beam, we have

$$D_x^{(0)} = \begin{cases} 2\pi\lambda \exp(-x) & x > 0 \\ -2\pi\lambda \exp(x) & x < 0 \end{cases}. \tag{21}$$

Now we consider n_0 as given by Eq. (17). We apply perturbation theory and introduce ansatz

$$\begin{aligned} D_x &= D_x^{(0)} + gD_x^{(1)}, \\ D_y &= D_y^{(0)} + gD_y^{(1)}. \end{aligned} \tag{22}$$

Substituting Eqs. (22) and Eq. (17) into Eq. (19), equating terms of the same order and assuming for simplicity $x > 0$, we arrive at a set of equations for the corrections in the form

$$\begin{aligned} \frac{d^2}{dx^2} D_x^{(1)} &= D_x^{(1)} \pm 2\pi\lambda x \exp(\mp x), \\ \frac{d^2}{dx^2} D_y^{(1)} &= D_y^{(1)}. \end{aligned} \tag{23}$$

Corrections should vanish both at the infinity and near the source $D_{x,y}^{(1)}(x \to 0) = 0$ and $D_{x,y}(\pm\infty) = 0$, consequently,

$$\begin{aligned} D_x^{(1)} &= \mp\frac{\pi\lambda}{2} x(1 \pm x) \exp(\mp x), \\ D_y^{(1)} &= 0. \end{aligned} \tag{24}$$

Combining Eq. (21) with Eq. (24), we finally arrive at

$$\begin{aligned} D_x &= \pm 2\pi\lambda \exp(\mp x) \mp \frac{g\pi\lambda}{2} x(1 \pm x) \exp(\mp x), \\ D_y &= 0. \end{aligned} \tag{25}$$

Equation (25) fully defines the shock electromagnetic wave produced by the infinitely long (in y) line that propagates along the z axis.

IV. SHAPE OF THE PLASMA BUBBLE

A. Ballistic approximation

As the first step in our considerations, we neglect the effect of the plasma self-fields on the trajectories of the plasma electrons. This is the "ballistic" regime of plasma motion introduced in Ref. [13]; it assumes that the plasma electrons are moving with constant velocities.

We assume plasma electrons to be nonrelativistic and $v_{z0} \approx 1$, consequently for the upper half plane, we get

$$\frac{dx}{d\xi} \approx -2\pi\lambda \exp(-x_0) + \frac{g\pi\lambda}{2} x_0(1 + x_0) \exp(-x_0). \tag{26}$$

A solution to the equations above gives electron trajectories

$$x = x_0 - 2\pi\lambda\xi \exp(-x_0) + \frac{g\pi\lambda\xi}{2} x_0(1 + x_0) \exp(-x_0). \tag{27}$$

First, we consider the case of $g = 0$ and plot electron trajectories in Fig. 1 setting for the simplicity $\lambda = 1/2\pi$.

From Fig. 1, we observe that plasma flow has two regimes: laminar flow, when trajectories do not cross, and a two-stream flow. Switching point ξ_{sw} could be found from the following considerations: we consider the upper half plane ($x > 0$). The two-stream flow appears when the most inner electron trajectory crosses the next closest trajectory. This condition could be expressed as

$$-2\pi\lambda\xi_{sw} = \delta x_0 - 2\pi\lambda\xi_{sw} \exp(-\delta x_0). \tag{28}$$

Here δx_0 is the distance between starting points of the two trajectories. Solving for ξ_{sw} and assuming $\lambda < 0$, we get

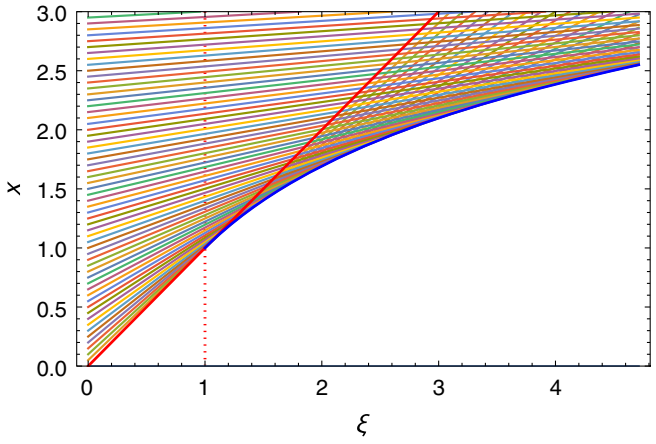

FIG. 1. Plasma flow in the ballistic approximation for the case of $|\lambda| = 1/2\pi$ and $g = 0$. The red line denotes the trajectory with $x_0 = 0$ [Eq. (32)], the blue line denotes the envelope of the two-stream flow given by Eq. (33), dashed line shows the switching point for the plasma flow.

$$\xi_{sw} = \frac{1}{2\pi|\lambda|}\frac{\delta x_0}{1-\exp(-\delta x_0)}. \tag{29}$$

Proceeding with the limit $\delta x_0 \to 0$, we finally have

$$\xi_{sw} = \frac{1}{2\pi|\lambda|}. \tag{30}$$

Before the switching point, the bubble has a linear "triangular" shape and the boundary is simply defined by the most inner trajectory

$$x_b = 2\pi|\lambda|\xi, \qquad \xi < \xi_{sw}. \tag{31}$$

The bubble boundary for the two-stream flow (for $\xi \geq \xi_{sw}$) can be found as an envelope for the plasma electron trajectories from the condition

$$\frac{dx}{dx_0} = 0, \tag{32}$$

and reads

$$x_b = 1 + \ln(2\pi|\lambda|\xi), \qquad \xi \geq \xi_{sw}. \tag{33}$$

Next, we account for the plasma gradient (now $g \neq 0$). The plasma flow still has two regimes, and the switching point now is found with the help of the condition

$$2\pi|\lambda|\xi_{sw} = \delta x_0 + 2\pi|\lambda|\xi_{sw}\exp(-\delta x_0) - \frac{g\pi|\lambda|\xi_{sw}}{2}\delta x_0(1+\delta x_0)\exp(-\delta x_0). \tag{34}$$

Solving for ξ_{sw}, we get

$$\xi_{sw} = \frac{1}{2\pi|\lambda|}\frac{\delta x_0}{1-\exp(-\delta x_0)+\frac{g}{4}\delta x_0(1+\delta x_0)\exp(-\delta x_0)}. \tag{35}$$

Proceeding with the limit $\delta x_0 \to 0$, we have

$$\xi_{sw} = \frac{1}{2\pi|\lambda|}. \tag{36}$$

We note that in the case of a small plasma gradient, the switching point remains at the same location as in the case of the uniform plasma and the first part of the plasma boundary remains the same as given by Eq. (32). It is worth mentioning that if $\lambda \ll 1$, then switching point $\xi_{sw} \to \infty$ and plasma flow is laminar. We note that in the case $g \neq 0$ boundary for the two-stream part of the flow could not be expressed in a simple form as Eq. (32) becomes a transcendental equation. However, the flow could be easily found numerically.

B. Small charge regime

Now we switch to a different approximation and account for the shielding effect. First, we derive a general expression for the force that acts on the plasma electrons. By combining Eq. (14) with Eq. (13) in the case of the nonrelativistic plasma electrons ($v_z \ll 1$), we get

$$\frac{dF_x}{dx} = n_i - n_e. \tag{37}$$

Integrating the equation above, we get

$$F_x(x) = \int_0^x (n_i - n_e)d\tilde{x} + F_x(0). \tag{38}$$

At rest, plasma is electrically neutral, so the total charge of the electrons and ions should be the same in both the lower ($x < 0$) and upper ($x > 0$) half-planes. As far as the charge is conserved, one may write $\int_0^\infty (n_i - n_e)d\tilde{x} = 0$, consequently, from Eq. (38), we have $F_x(\infty) = F_x(0)$. Lorentz force, F_x, has to vanish at the infinity, consequently, we conclude that $F_x(0) = 0$. With this observation, one may rewrite Eq. (38) as

$$F_x(x) = \int_0^x (n_i - n_e)d\tilde{x}. \tag{39}$$

We notice that if the two-stream regime does not develop, then the shape of the bubble is always defined by the most inner trajectory of the plasma electron that starts at $x_0 = 0$. A force that acts on this electron from the side of the plasma ions is found from Eq. (39) with $n_e = 0$ (inside the bubble there are no electrons). For the unperturbed case of $g = 0$, we get a familiar expression of the ion focusing force

$$F_x^i = x, \qquad x \le x_b. \tag{40}$$

We note that we defined F_x as a force per unit charge, consequently, the force that acts on the plasma electron is recovered by multiplying F_x by the charge of the plasma electron. In our notations, it is simply -1.

Using initial conditions $x_0 = 0$ and $V_0 = -2\pi\lambda$, one can arrive at the expression for the bubble shape in the form

$$x_b = 2\pi|\lambda|\sin(\xi). \tag{41}$$

The range of validity for the formula above could be established from the condition of the crossing of the two closest trajectories and, following the same steps as in the ballistic approximation, one can deduce the equation for the switching point in the form

$$\sin(\xi_{sw}) = \frac{1}{2\pi|\lambda|}. \tag{42}$$

For this equation to have no real solutions for the ξ_{sw}, the inequality $\sin(\xi_{sw}) > 1$ must hold, consequently,

$$|\lambda| < \frac{1}{2\pi}. \tag{43}$$

The condition above sets the upper limit on the line charge density for the plasma flow to be laminar and is described by Eq. (41).

Next, we notice that if the condition (43) significantly fulfilled, then small perturbation to the ion and electron densities as well as to the ion force should not induce a two-stream regime and the plasma flow should remain laminar. Consequently, one may account for the ion density gradient

$$n_i = 1 + gx, \tag{44}$$

with the help of Eq. (39), we get

$$F_x^i = x + g\frac{x^2}{2}, \qquad x \le x_b. \tag{45}$$

As far as the bubble boundary is given by the most inner electron trajectory, the equation for the bubble boundary reads

$$\frac{d^2x_b}{d\xi^2} = -x_b - g\frac{x_b^2}{2}, \tag{46}$$

with initial conditions $x_b(0) = 0$ and $x_b'(0) = 2\pi\lambda$. Equation (46) could be solved using the perturbation method and solution up to the terms of the order $\mathcal{O}[g^2]$ reads

$$x_b = 2\pi|\lambda|\sin(\xi) - \frac{8\pi^2\lambda^2}{3}g\left[\sin\left(\frac{\xi}{2}\right)\right]^4. \tag{47}$$

From Eq. (42), we observe that in the case of the laminar flow and without the plasma gradient, bubble shape is universal and scales linearly with the charge. However, in the case of the plasma gradient, as follows from Eq. (47), bubble shape always depends on the charge. Introducing normalized variable $x_b^n = x_b/(2\pi|\lambda|)$, we arrive at the final bubble shape in the form

$$x_b^n = \sin(\xi) - g\frac{4\pi|\lambda|}{3}\left[\sin\left(\frac{\xi}{2}\right)\right]^4. \tag{48}$$

We conclude that the transverse plasma gradient results in the "bending" of the bubble toward the less dense plasma. Qualitatively, this asymmetry is proportional to the product of the driver charge density and the strength of the plasma gradient.

V. PLASMA FLOW AND PLASMA DENSITY

Immediately behind the driver, at $\xi = 0^+$, the plasma density n_0 is given by Eq. (17).

If we assume that electron trajectories are known, then from the continuity of the plasma flow, we conclude that

$$n_e(x, y, \xi)dS = n_0(x_0, y_0)dS_0 \tag{49}$$

from which it follows that

$$n_e(x, y, \xi) = n_0(x_0, y_0)\frac{dS_0}{dS}. \tag{50}$$

Accounting for the translation symmetry in y, we simply have

$$n_e(x, \xi) = n_0(x_0)\frac{dx_0}{dx}, \tag{51}$$

or, substituting n_0 from Eq. (17), we get

$$n_e(x, \xi) = (1 + gx_0)\frac{dx_0}{dx}. \tag{52}$$

We note that if plasma flow is laminar (electron trajectories do not cross), then the force that is associated with the plasma electrons can be easily found with the help of Eq. (39) and with Eq. (52) reads

$$F_x^e = -\int_0^x (1 + gx_0)\frac{dx_0}{dx}dx = -x_0(x) - g\frac{x_0(x)^2}{2}. \tag{53}$$

Interestingly, this leads to a closed form solution for electron trajectories as the equation of motion for each plasma electron with initial conditions $x(0) = x_0$ and $x'(0) = -D_x(x_0)$ now reads

$$\frac{d^2x}{d\xi^2} = -x - g\frac{x^2}{2} + x_0 + g\frac{x_0^2}{2}. \tag{54}$$

The equation above can be again solved using the perturbation approach:

$$x = x^{(0)} + gx^{(1)} + \mathcal{O}(g^2). \tag{55}$$

With Eq. (25), the equation for the leading order $x^{(0)}$ reads

$$\begin{aligned} \frac{d^2x^{(0)}}{d\xi^2} &= -x^{(0)} + x_0, \\ x^{(0)}(0) &= x_0, \\ \left.\frac{dx^{(0)}}{d\xi}\right|_{\xi=0} &= \pm 2\pi|\lambda| \exp(\mp x_0). \end{aligned} \tag{56}$$

Here the upper sign is for the case of $x > 0$ and the lower sign is for the case of $x < 0$. Solution to this equation reads

$$x^{(0)} = x_0 \pm 2\pi|\lambda| \exp(\mp x_0)\ \sin(\xi). \tag{57}$$

Next to the leading order $x^{(1)}$ could be found by substituting Eq. (55) with Eq. (25) into Eq. (54) and equating terms of the same order. After some algebra, we have

$$\begin{aligned} \frac{d^2x^{(1)}}{d\xi^2} &= -x^{(1)} - \frac{(x^{(0)})^2}{2} + \frac{x_0^2}{2}, \\ x^{(1)}(0) &= 0, \\ \left.\frac{dx^{(1)}}{d\xi}\right|_{\xi=0} &= \mp\frac{\pi|\lambda|}{2} x_0(1 \pm x_0) \exp(\mp x_0). \end{aligned} \tag{58}$$

After substituting Eq. (57) into Eq. (58), the expression for the $x^{(1)}$ is found to be

$$\begin{aligned} x^{(1)} = &-\frac{8\pi^2|\lambda|^2}{3} \exp(\mp 2x_0)\left[\sin\left(\frac{\xi}{2}\right)\right]^4 \\ &\pm \pi|\lambda| x_0 \xi \exp(\mp x_0)\cos(\xi) \\ &\mp \frac{\pi|\lambda| x_0}{2} \exp(\mp x_0)[3 \pm x_0]\sin(\xi). \end{aligned} \tag{59}$$

Combining Eqs. (57) and (59) with the help of Eq. (55), we plot electron trajectories in Fig. 2 (left panel) for the case $g = 0.2$ (highly inhomogeneous plasma density) and $|\lambda| = 0.6/2\pi$. The numbers in the example are chosen to emphasize the effect visually and are exaggerated in comparison to common realistic parameters. As expected, the flow is laminar and modification to the bubble shape is small (of the order $\sim\lambda^2 g$) as dictated by Eq. (47).

To examine the total plasma density $n(x,\xi) = n_i(x,\xi) - n_e(x,\xi)$, we compare several cases [$n(x,\pi/8)$, $n(x,\pi/4)$ and $n(x,\pi/2)$] in Fig. 3. The plot is produced

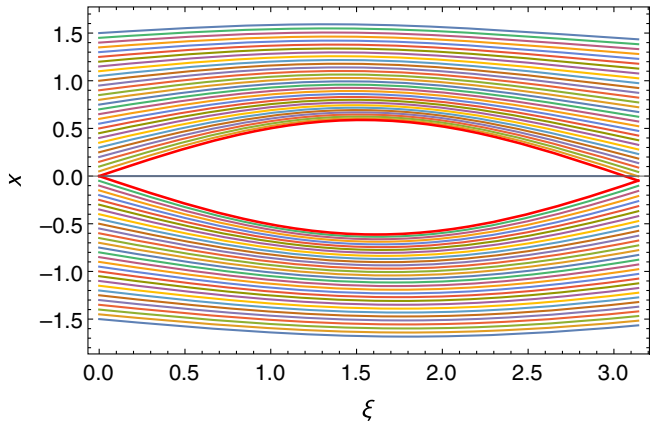

FIG. 2. Plasma flow in the approximation of a small charge for the case of $\lambda = 0.6/2\pi$ and $g = 0.2$ (numbers are chosen to emphasize the effect visually). Thick red lines denote bubble boundary.

with the help of Eq. (52). As far as the flow is laminar, the solution to Eq. (55), with Eqs. (57) and (59), is unique with respect to x_0 for a given x and could be found numerically. Consequently, one may derive an explicit expression for the plasma density in terms of x_0 and, using this numerical solution, compute $n(x_0(x),\xi)$. We do not provide final expressions as they are bulky but can easily be produced once needed.

As could be seen from Fig. 3, in contrast to the cylindrically symmetric case (see Ref. [13]), plasma density does not have a singularity at the plasma boundary. However, it has a jump that corresponds to the jump in the electron density. We observe, that, as expected, the jump in the electron density increases toward the bubble wall and is maximal at the bubble boundary.

In Fig. 4, we plot plasma density close to the end of the bubble $\xi = 3\pi/4$ where the witness beam is placed to maximize the acceleration rate. One can observe that an initial seed in plasma density gradient $g = 0.2$ results in a

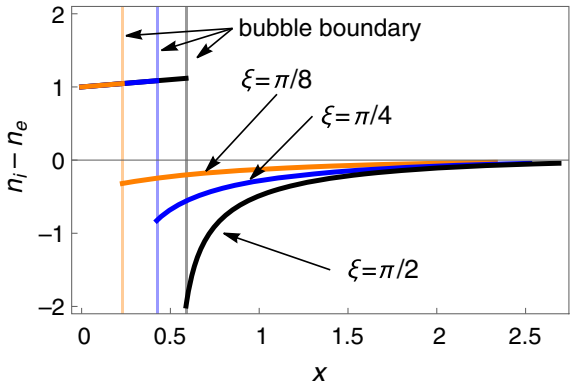

FIG. 3. Total plasma density for the case of $x > 0$ and three different values of ξ inside the bubble electron density n_e is equal to zero and the total density is essentially ion density given by Eq. (44). $|\lambda| = 0.6/2\pi$ and $g = 0.2$.

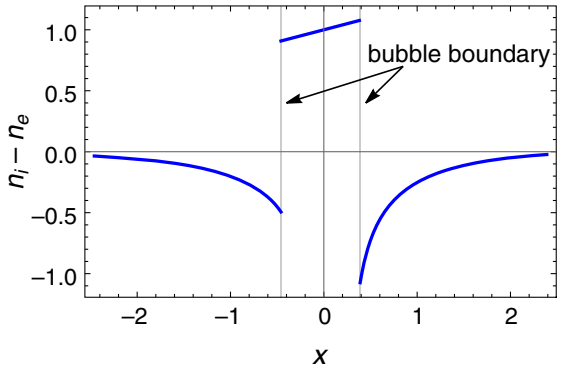

FIG. 4. Total plasma density for the case of $\xi = 3\pi/4$, $|\lambda| = 0.6/2\pi$, and $g = 0.2$.

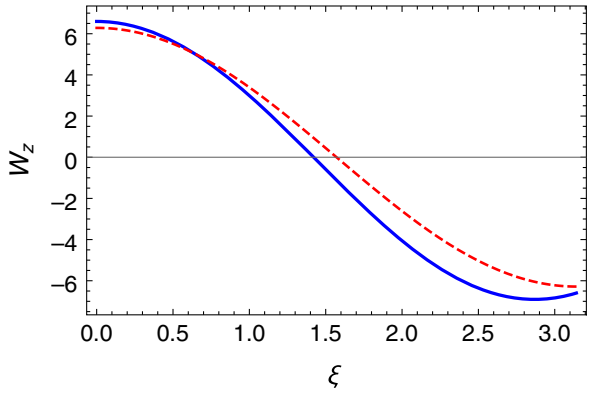

FIG. 5. Longitudinal wake potential per unit length $W_z = -E_z/\lambda$ for the case $|\lambda| = 0.6/2\pi$, $g = 0.2$ (blue line), and $g = 0$ (red dashed line).

significant imbalance of the total plasma density at the bubble boundary. This, in turn, may result in the asymmetry of the witness self wake and consequently may affect the emittance of the witness beam.

VI. WAKEFIELD

It was established in Sec. IV B that, in the small charge regime, a flat driver does not produce any transverse wake even in the case of nonhomogeneous plasma. The Lorentz force inside the bubble is a focusing force given by Eq. (45). Combining the first and second formulas in Eq. (13), we get

$$\frac{dE_z}{dx} = -\frac{dF_x}{d\xi}. \tag{60}$$

The expression above is widely known as the Panofsky-Wenzel theorem (see Refs. [44,45]) From Eq. (61), we immediately conclude that E_z is constant inside the bubble and depends on ξ only.

Substitution of Eq. (38) into Eq. (61) gives

$$\frac{dE_z}{dx} = -\frac{dF_x^e}{d\xi}, \tag{61}$$

with F_x^e, given by Eq. (53). Expanding the ξ derivative on the right-hand side and integrating over x, we get for the E_z inside the bubble

$$E_z = \int_{x_b}^{\infty} \frac{dx_0}{dx}\frac{dx}{d\xi}dx + g\int_{x_b}^{\infty} x_0 \frac{dx_0}{dx}\frac{dx}{d\xi}dx. \tag{62}$$

Interestingly, both integrals in the expression evaluate explicitly. Indeed, switching from integration over x to integration over x_0, we get

$$E_z = \int_0^{\infty} \frac{dx(x_0)}{d\xi}dx_0 + g\int_0^{\infty} x_0 \frac{dx(x_0)}{d\xi}dx_0, \tag{63}$$

with $x(x_0)$ defined through Eq. (55) and $x^{(0)}$ and $x^{(1)}$ given by Eqs. (57) and (59), respectively.

After some algebra, we finally get

$$E_z = -2\pi\lambda\cos(\xi) - g\pi\lambda\left[\frac{\cos(\xi)}{2} + \sin(\xi) \times \left[\frac{2\pi\lambda}{3} - \frac{2}{3}\pi\lambda\cos(\xi) - \xi\right]\right]. \tag{64}$$

We observe that if the plasma is homogeneous, then the expression for the electric field despite the bubble formation is exactly the same as in the linear plasma response case. When there is a slight transverse density gradient $\sim g$ in plasma, the nonlinearity of the same magnitude perturbs the longitudinal wake potential W_z (see Fig. 5). We reiterate two conclusions. In the case of a laminar plasma flow, an infinitely flat driver does not produce any transverse wake even if the local plasma density fluctuates from the equilibrium. In the laminar regime of the plasma flow in the flat case, the longitudinal component of the electric field E_z generated by the driver is constant inside the bubble and in the case of a homogeneous plasma has the same harmonic form as in the case of the linear plasma response.

VII. CONCLUSION

We have suggested a simple model of the flat bubble formation by the flat driver beam. Using this model and ballistic approximation, introduced in Ref. [13], we have demonstrated that in the case of the flat drive, two different regimes (laminar and turbulent) can develop. The switching point where one type of flow switches to another depends solely on the line charge density of the driver.

We have investigated the laminar plasma flow regime generated by the flat electron driver. We demonstrated that a small perturbation to the plasma density results in

"bending" of the bubble toward a lower plasma gradient. Despite such a modification to the bubble shape and symmetry breaking, in the case of the nonrelativistic plasma flow, the wake generated by the flat driver does not have any deflecting components. The focusing force of the ion column has the same gradient as the initial gradient of the plasma density. It is worth mentioning that this gradient is independent of the longitudinal coordinate ξ and consequently should not affect the emittance of the accelerated beam. The model and its extensions could be applied to the analysis of the flat beam injection into the plasma cell —an ongoing project at the AWA facility [43].

We note that numerical examples, provided in the paper, are synthetic, and we choose parameters for these examples for the illustrative purpose only. In reality, the parameter g—a transverse plasma gradient should be on the order of 1% or less. We note that the model most probably breaks when $\lambda \sim \frac{1}{2\pi}$ and bubble radius is ~0.5 as at this point, plasma electrons are most likely to become relativistic.

In a realistic scenario, when the driver has a finite flatness $\sigma_x/\sigma_y > 0$, the edge effects that come from the finite driver size in y must be considered. As was pointed out in Ref. [37], for a finite flat driver inside the vacuum channel, along with the dipole wake, there always exists a quadrupole wake that may result in a quadrupole instability. While the present study shows that in the limiting case of $\sigma_x/\sigma_y = 0$ in the laminar bubble regime, both wakes are suppressed completely, scaling of these wakes with the beam ellipticity $\chi = \sigma_y/\sigma_x$ is an open question. Nonetheless, the observed analogy between the flat beam in a slab channel and a flat beam forming a flat bubble opens potentially new opportunities to combat hosing instability.

Presented formalism is complementary to the well-known analytical Lu model of the plasma bubble Refs. [12,15]. While the Lu equation works best when the bubble radius is significantly larger than the plasma wavelength, the presented model and approach of the Ref. [13] works in the opposite limit when the bubble size is way smaller than the plasma wavelength. The ballistic model and the small charge model may serve as an initial condition for the Lu equation. A potential next step is an attempt to merge these models such that the combined model will cover the whole parameter range.

In contrast to the approach of Ref. [13], the present model, due to the different geometry, does not contain singularities at the position of the driver and the plasma boundary. This results in the formation of the transition region from the laminar flow to the two-stream turbulent flow. In reality, even in the case of the round driver, the field is always finite at the driver position, consequently, similar effects should occur. Namely, in the round case, there might exist a transition of the laminar flow to the turbulent flow. In the case of the laminar flow in the cylindrical geometry for the round driver, the wake and its response to the external perturbation are expected to be different.

ACKNOWLEDGMENTS

The author is grateful to G. Stupakov for fruitful discussions. The work was supported by the Government of the Russian Federation through the ITMO Fellowship and Professorship Program.

[1] G. A. Voss and T. Weiland, The wake field acceleration mechanism, DESY Report No. 82-074, 1982.
[2] Pisin Chen, J. M. Dawson, Robert W. Huff, and T. Katsouleas, Acceleration of Electrons by the Interaction of a Bunched Electron Beam with a Plasma, Phys. Rev. Lett. **54**, 693 (1985).
[3] J. B. Rosenzweig, Nonlinear Plasma Dynamics in the Plasma Wake-Field Accelerator, Phys. Rev. Lett. **58**, 555 (1987).
[4] J. B. Rosenzweig, B. Breizman, T. Katsouleas, and J. J. Su, Acceleration and focusing of electrons in two-dimensional nonlinear plasma wake fields, Phys. Rev. A **44**, R6189 (1991).
[5] Spencer Gessner *et al.*, Path towards a beam-driven plasma linear collider, Snowmass-21, Letter of Interest, 2020, No. available at https://www.snowmass21.org/docs/files/summaries/AF/SNOWMASS21-AF6_AF4-168.pdf.
[6] Eric R. Colby and L. K. Len, Roadmap to the future, Rev. Accel. Sci. Techol. **09**, 1 (2016).
[7] ALEGRO Collaboration, Towards an advanced linear international collider, arXiv:1901.10370.
[8] Erik Adli, Plasma wakefield linear colliders—Opportunities and challenges, Phil. Trans. R. Soc. A **377**, 20180419 (2019).
[9] Alex Murokh, Pietro Musumeci, Alexander Zholents, and Stephen Webb, Towards a compact high efficiency FEL for industrial applications, in *Proceedings of the OSA High-brightness Sources and Light-driven Interactions Congress 2020 (EUVXRAY, HILAS, MICS)* (Optica Publishing Group, Washington, DC, 2020), paper EF1A.3.
[10] J. B. Rosenzweig *et al.*, An ultra-compact x-ray free-electron laser, New J. Phys. **22**, 093067 (2020).
[11] N. Barov, J. B. Rosenzweig, M. C. Thompson, and R. B. Yoder, Energy loss of a high-charge bunched electron beam in plasma: Analysis, Phys. Rev. ST Accel. Beams **7**, 061301 (2004).
[12] W. Lu, C. Huang, M. Zhou, W. B. Mori, and T. Katsouleas, Nonlinear Theory for Relativistic Plasma Wakefields in the Blowout Regime, Phys. Rev. Lett. **96**, 165002 (2006).
[13] G. Stupakov, B. Breizman, V. Khudik, and G. Shvets, Wake excited in plasma by an ultrarelativistic pointlike bunch, Phys. Rev. Accel. Beams **19**, 101302 (2016).
[14] G. Stupakov, Short-range wakefields generated in the blowout regime of plasma-wakefield acceleration, Phys. Rev. Accel. Beams **21**, 041301 (2018).
[15] T. N. Dalichaouch, X. L. Xu, A. Tableman, F. Li, F. S. Tsung, and W. B. Mori, A multi-sheath model for highly nonlinear plasma wakefields, Phys. Plasmas **28**, 063103 (2021).
[16] C. Huang, V. K. Decyk, C. Ren, M. Zhou, W. Lu, W. B. Mori, J. H. Cooley, T. M. Antonsen, and T. Katsouleas,

QUICKPIC: A highly efficient particle-in-cell code for modeling wakefield acceleration in plasmas, J. Comput. Phys. **217**, 658 (2006).

[17] J.-L. Vay, D. P. Grote, R. H. Cohen, and A. Friedman, Novel methods in the particle-in-cell accelerator code-framework warp, Comput. Sci. Discovery **5**, 014019 (2012).

[18] R. A. Fonseca, L. O. Silva, F. S. Tsung, V. K. Decyk, W. Lu, C. Ren, W. B. Mori, S. Deng, S. Lee, T. Katsouleas, and J. C. Adam, Osiris: A three-dimensional, fully relativistic particle in cell code for modeling plasma based accelerators, in *Computational Science—ICCS 2002*, edited by Peter M. A. Sloot, Alfons G. Hoekstra, C. J. Kenneth Tan, and Jack J. Dongarra (Springer, Berlin, Heidelberg, 2002), pp. 342–351.

[19] S. Kuschel, D. Hollatz, T. Heinemann, O. Karger, M. B. Schwab, D. Ullmann, A. Knetsch, A. Seidel, C. Rödel, M. Yeung, M. Leier, A. Blinne, H. Ding, T. Kurz, D. J. Corvan, A. Sävert, S. Karsch, M. C. Kaluza, B. Hidding, and M. Zepf, Demonstration of passive plasma lensing of a laser wakefield accelerated electron bunch, Phys. Rev. Accel. Beams **19**, 071301 (2016).

[20] J. P. Couperus, R. Pausch, A. Köhler, O. Zarini, J. M. Krämer, M. Garten, A. Huebl, R. Gebhardt, U. Helbig, S. Bock, K. Zeil, A. Debus, M. Bussmann, U. Schramm, and A. Irman, Demonstration of a beam loaded nanocoulomb-class laser wakefield accelerator, Nat. Commun. **8**, 487 (2017).

[21] M. Tzoufras, W. Lu, F. S. Tsung, C. Huang, W. B. Mori, T. Katsouleas, J. Vieira, R. A. Fonseca, and L. O. Silva, Beam Loading in the Nonlinear Regime of Plasma-Based Acceleration, Phys. Rev. Lett. **101**, 145002 (2008).

[22] T. J. Mehrling, R. A. Fonseca, A. Martinez de la Ossa, and J. Vieira, Mitigation of the Hose Instability in Plasma-Wakefield Accelerators, Phys. Rev. Lett. **118**, 174801 (2017).

[23] T. J. Mehrling, C. Benedetti, C. B. Schroeder, E. Esarey, and W. P. Leemans, Suppression of Beam Hosing in Plasma Accelerators with Ion Motion, Phys. Rev. Lett. **121**, 264802 (2018).

[24] R. Lehe, C. B. Schroeder, J.-L. Vay, E. Esarey, and W. P. Leemans, Saturation of the Hosing Instability in Quasi-linear Plasma Accelerators, Phys. Rev. Lett. **119**, 244801 (2017).

[25] C. Huang *et al.*, Hosing Instability in the Blow-Out Regime for Plasma-Wakefield Acceleration, Phys. Rev. Lett. **99**, 255001 (2007).

[26] Carl A. Lindstrøm, Staging of plasma-wakefield accelerators, Phys. Rev. Accel. Beams **24**, 014801 (2021).

[27] Chunguang Jing, Dielectric wakefield accelerators, Rev. Accel. Sci. Techol. **09**, 127 (2016).

[28] A. Siy, N. Behdad, J. Booske, M. Fedurin, W. Jansma, K. Kusche, S. Lee, G. Mouravieff, A. Nassiri, S. Oliphant, S. Sorsher, K. Suthar, E. Trakhtenberg, G. Waldschmidt, and A. Zholents, Fabrication and testing of corrugated waveguides for a collinear wakefield accelerator, Phys. Rev. Accel. Beams **25**, 021302 (2022).

[29] A. Zholents, S. Baturin, S. Doran, W. Jansma, M. Kasa, R. Kustom, A. Nassiri, J. Power, K. Suthar, E. Trakhtenberg, I. Vasserman, G. Waldschmidt, and J. Xu, A compact wakefield accelerator for a high repetition rate multi user x-ray free-electron laser facility, in *Proceedings of the Conference on High-Brightness Sources and Light-driven Interactions* (Optica Publishing Group, Washington, DC, 2018), paper EW3B.1.

[30] David H. Whittum, William M. Sharp, Simon S. Yu, Martin Lampe, and Glenn Joyce, Electron-Hose Instability in the Ion-Focused Regime, Phys. Rev. Lett. **67**, 991 (1991).

[31] C. Li, W. Gai, C. Jing, J. G. Power, C. X. Tang, and A. Zholents, High gradient limits due to single bunch beam breakup in a collinear dielectric wakefield accelerator, Phys. Rev. ST Accel. Beams **17**, 091302 (2014).

[32] S. S. Baturin and A. Zholents, Stability condition for the drive bunch in a collinear wakefield accelerator, Phys. Rev. Accel. Beams **21**, 031301 (2018).

[33] E. I. Simakov, G. Andonian, S. S. Baturin, and P. Manwani, Limiting effects in drive bunch beam dynamics in beam-driven accelerators: Instability and collective effects, J. Instrum. **17**, P05013 (2022).

[34] P. Piot, Y.-E Sun, and K.-J. Kim, Photoinjector generation of a flat electron beam with transverse emittance ratio of 100, Phys. Rev. ST Accel. Beams **9**, 031001 (2006).

[35] J. Zhu, P. Piot, D. Mihalcea, and C. R. Prokop, Formation of compressed flat electron beams with high transverse-emittance ratios, Phys. Rev. ST Accel. Beams **17**, 084401 (2014).

[36] A. Halavanau, J. Hyun, D. Mihalcea, P. Piot, T. Sen, and J. C. T. Thangaraj, Magnetized and Flat Beam Experiment at FAST, in *Proceedings of International Particle Accelerator Conference, IPAC-2017, Copenhagen, Denmark, 2017* (JACoW, Geneva, Switzerland, 2017), pp. 3876–3879.

[37] S. S. Baturin, G. Andonian, and J. B. Rosenzweig, Analytical treatment of the wakefields driven by transversely shaped beams in a planar slow-wave structure, Phys. Rev. Accel. Beams **21**, 121302 (2018).

[38] A. Tremaine, J. Rosenzweig, and P. Schoessow, Electromagnetic wake fields and beam stability in slab-symmetric dielectric structures, Phys. Rev. E **56**, 7204 (1997).

[39] Brendan D. O'Shea, Gerard Andonian, S. S. Baturin, Christine I. Clarke, P. D. Hoang, Mark J. Hogan, Brian Naranjo, Oliver B. Williams, Vitaly Yakimenko, and James B. Rosenzweig, Suppression of Deflecting Forces in Planar-Symmetric Dielectric Wakefield Accelerating Structures with Elliptical Bunches, Phys. Rev. Lett. **124**, 104801 (2020).

[40] Shiyu Zhou, Jianfei Hua, Weiming An, Warren B. Mori, Chan Joshi, Jie Gao, and Wei Lu, High Efficiency Uniform Wakefield Acceleration of a Positron Beam Using Stable Asymmetric Mode in a Hollow Channel Plasma, Phys. Rev. Lett. **127**, 174801 (2021).

[41] Spencer Gessner *et al.*, Demonstration of a positron beam-driven hollow channel plasma wakefield accelerator, Nat. Commun. **7**, 11785 (2016).

[42] Spencer J. Gessner, Demonstration of the hollow channel plasma wakefield accelerator, Ph.D. thesis, Stanford University, 2016.

[43] P. Manwani, H. S. Ancelin, G. Andonian, G. Ha, J. G. Power, J. B. Rosenzweig, and M. Yadav, Asymmetric beam driven plasma wakefields at the AWA, in *Proceedings of the 12th International Particle Accelerator Conference, IPAC'21, Campinas, SP, Brazil* (JACoW, Geneva, Switzerland, 2021), pp. 1732–1735, 10.18429/JACoW-IPAC2021-TUPAB147.

[44] W. K. H. Panofsky and W. A. Wenzel, Some considerations concerning the transverse deflection of charged particles in radio frequency fields, Rev. Sci. Instrum. **27**, 967 (1956).

[45] Alex Chao, *Physics of Collective Beam Instabilities in High Energy Accelerators* (Wiley and Sons, New York, 1993).